Analysis of Ferromagnetic-Multiferroic Interfaces in Epitaxial Multilayers of LSMO and BFO

Author: Peter Knapp
Department of Mechanical Engineering, Northwestern University, Chicago, IL 60201

Advisor: Professor Jeremiah Abiade
Department of Mechanical Engineering, University of Illinois at Chicago, Chicago, IL 60607

Abstract – Bilayers were fabricated from ferromagnetic LSMO (Lanthanum Strontium Manganate Oxide, $La_{0.7}Sr_{0.3}MnO_3$) and ferroelectric BFO (Bismuth Ferrite, $BiFeO_3$) using pulsed laser deposition in the presence of O_2 on $LaAlO_3$ and $SrTiO_3$ substrates. The layer thickness and the layer order were varied among 16 samples. The bilayers were analyzed using TEM, XRD, XRR, and XPS to determine the stoichiometry, interlayer diffusion, roughness, and other structural features. TEM imaging showed that portions of the bilayers were highly crystalline. However, XRD analysis demonstrated that the majority of films were amorphous, with some polycrystalline and nanocrystalline samples. XRR data indicated a high roughness but did not yield good thickness values. Finally, XPS confirmed that material stoichiometry was preserved. It appears that the deposition process still needs optimization. This research will serve as the basis for future experiments on the magnetic properties of LSMO/BFO bilayers.

Keywords – Pulsed Laser Deposition, X-Ray Diffraction, LSMO, BFO, Multiferroic Heterostructures, Perovskite

Introduction – Traditionally, ferroelectric and ferromagnetic materials have been used for actuators, optoelectronic devices, capacitors, information storage devices, and sensors.[1] However, recently, multiferroic materials, materials which demonstrate both magnetic and ferroelectric properties, have piqued great interest. This unique combination of ferromagnetic and ferroelectric ordering means these materials have a wide range of potential uses for which standard ferromagnetic and ferroelectric materials are not ideally suited.[2] In multiferroic materials, electric polarization can be used to influence ferromagnetic polarization, thereby manipulating magnetization and ferromagnetic ordering.[1] Multilayer heterostructures of these materials are of particular interest, because they allow for control of electron spin polarization which has a number of applications in the area of magnetic sensors and devices. Further research into and development of these novel heterostructures could demonstrate unusual uses only appropriate for these materials.[1,2] It is believed that the end result of this research

will be the realization of multicomponent multiferroic systems which afford electrical control of magnetism.

Contemporary research in this area has focused on thin film, hetero-epitaxial bilayers, of ferromagnetic (FM) and antiferromagnetic (AFM) materials.[3] These bilayers exhibit three distinctive phenomena which merit further research: exchange bias (EB), exchange enhancement (EE), and exchange coupling (EC). Exchange bias is a shift of the hysteresis loop of a material along the field axis, in the case of FM/AFM, specifically $La_{0.67}Sr_{0.33}MnO_3$ /$SrRuO_3$ bilayers in the positive direction. EB is a result of the alignment and coupling of the interfacial spin states between the antiferromagnetic and ferromagnetic layers of the system.[3] Exchange enhancement is an augmentation of the coercive field of the ferromagnetic layer as a result of exchange interaction.[4,5] Finally, exchange coupling is an interaction between the spin states of the atoms in between the ferromagnetic and anti-ferromagnetic layers; it is the base effect that allows for EB and EE.[2] These phenomena are extremely important in the development of multiferroic bilayers.

The pairing of ferromagnetic lanthanum strontium manganite oxide ($La_{0.7}Sr_{0.3}MnO_3$, LSMO), with multiferroic, ferroelectric bismuth ferrite ($BiFeO_3$, BFO) has merited considerable study.[1-3,5] On its own LSMO possesses a high Curie Temperature of 370 K and interesting colossal magneto resistance properties which are active at and above room temperature making it an ideal candidate for research.[1] LSMO is a rare earth manganite which, with hole doping, becomes a member of an intriguing family of conductive and ferromagnetic materials which have potential uses as memory materials, sensors, and as electrodes in ferroelectric films.[1,5] Similarly, BFO has been the subject of research because it is ferroelectric and anti-ferromagnetic with a high Curie temperature of 537 K and a high Néel temperature of 107 K.[5] The combination of a high Curie and Néel temperature allows for coupling of magnetic and electrical orders at high temperatures making BFO a promising material for the development of multiferroic technologies; the most prominent being tunnel junction devices based on

thin films of BFO.[1,5] Studies on bilayers of BFO and LSMO are advantageous, especially when compared to earlier studies focusing on bilayers of transition metal anti-ferromagnetic alloys and metallic ferromagnets, because they are both perovskites and have similar lattice parameters, 0.396 nm for BFO and 0.387 nm for LSMO.[1,3] This allows for very close control of film growth, ensuring the multilayers are epitaxial which is integral to the investigation of the exchange effects between the ferromagnetic and anti-ferromagnetic layers. Additionally, bilayers are grown on substrates that possess a perovskite structure to further insure uniform crystalline structure throughout. The most commonly used substrates are Lanthanum Aluminate ($LaAlO_3$) and Strontium Titanate ($SrTiO_3$).[3]

As of yet, researchers know very little about how complex interfacial phenomena between layers of the film affect magnetic properties.[1,6-7] It is necessary to understand how local types of interference at layer boundaries including diffusion of chemical species, deviations from stoichiometry, and lattice mismatch resulting from different lattice parameter between the FM and AFM layer effect bilayer properties in order to fully characterize these heterostructures and utilize them in novel technologies.[6,7] This paper reports on experiments to determine how varying bilayer parameters effect interfacial interactions. First, the substrate on which the bilayers are grown will be varied between $LaAlO_3$ and $SrTiO_3$. Second, the thickness of the BFO and LSMO layers will be varied to determine which components of the bilayer dominate in interfacial interaction. Finally the order in which the layers are deposited will be varied in order to fully characterize component interaction. These experiments will hopefully serve as the basis for future research into the magnetic interaction of LSMO and BFO bilayers.

Films will be grown using Pulsed Laser Deposition and will be characterized by transmission electron microscopy (TEM), x-ray reflectivity (XRR) and diffraction (XRD) techniques, and x-ray photoelectron spectroscopy (XPS). Pulsed laser deposition is used because it is inexpensive and ideal for the deposition of complex oxides as it preserves stoichiometry and can be performed in the presence of a background gas such as O_2, insuring proper film growth.[8] Transmission electron microscopy probes the

local crystal structure, and provides evidence about the crystalline phase of the film and alignment between layers of the film. X-ray reflectivity and diffraction techniques are used for analysis as they provide a detailed electron density profile which can be used to judge film characteristics, the most important being the crystallinity of the whole film, the thickness of the FM and AFM layers, lattice mismatch, and diffusion of one component into another. Finally, XPS probes the composition of certain areas of the surface of the film, and can be used to determine the changes in stoichiometry between the target material and the deposited layer.

Materials and Methods – 5mmx5mmx0.5mm silicon, quartz, $LaAlO_3$ (100)k, and $SrTiO_3$ (100)k substrates with one side polished, and a miscut of 0^o manufactured by CrysTec were used in all experiments. $BiFeO_3$ and $La_{0.7}Sr_{0.3}MnO_3$ rotating rod targets, manufactured by Kurt J. Lesker, were used in all experiments. These targets were constructed from pre-synthesized oxide powders using a low stress powder compression technique. Pulsed laser deposition was carried out using a pulsed KrF excimer laser with an output wavelength of 248 nm and a pulse duration of 15 ns.

Before beginning film deposition, the growth rate of perovskite films on a perovskite substrate in the available PLD setup was determined. $LaAlO_3$, Silicon, and Quartz substrates were layered on one another so as to form steps. Layering substrates on top of on another means portions of the substrate surface are protected from depositing material and no film forms there, and at the boundary between the protected and unprotected surface a plateau forms, which can be measured in order to determine the thickness of the deposited film. The substrates were them mounted on the deposition stage. A sanded and polished LSMO target was mounted in the vacuum chamber. The chamber was sealed and vacuum pumped until the pressure reached $5*10^{-4}$ Torr. The substrates were heated to 650^o C over a period of 30 minutes and the target was pre-ablated for 500 pulses. Once the substrate reached the target temperature background O_2 gas was introduced at a pressure of 10^{-2} Torr and 12,000 pulses of LSMO were deposited with a shot frequency of 5 Hz and a laser fluence of 1.5 Jcm^{-2}. The distance

between target and substrate was 4.5 cm. Following the deposition, vacuum was reestablished and the substrate was allowed to cool to room temperature over 1.5 hours. The substrates were removed, separated, and sonicated in acetone and methanol to wash off any adhesive. Film thickness was measured using a stylus profilometer and divided by the number of pulses to determine the growth rate, which was 0.014 nm/pulse. This growth rate can be applied to all substrates and targets as only perovskite type materials are used and all deposition parameters are held constant.

For the actual depositions, targets were sanded and polished at room temperature and substrates were sonicated for 5 minutes in acetone, then 5 minutes in methanol. Substrates were affixed with silver paint glue either directly to the deposition stage, or on a rotating sample mount that allowed for deposition on multiple substrates without breaking vacuum. Targets were pre-ablated for 500 pulses at a pressure of $5*10^{-4}$ Torr. Substrates were heated to 650^{o} Celsius over a thirty minute period. High temperatures insure epitaxial film growth; the slow heating prevents the buildup of thermal stresses which could damage the substrate. The substrate was held at 650^{o} Celsius for the entire deposition process. Once the ablation temperature was reacted O_2 gas was introduced at a pressure of 10^{-2} Torr, this pressure that was maintained throughout deposition. The laser was pulsed at a frequency of 5Hz with a laser fluence of 1.5 $J*cm^{-2}$. The distance between target and substrate was 4.5 cm. Following deposition, the O_2 supply was removed and pressure lowered to $5*10^{-4}$ Torr. The substrate was then cooled to room temperature over a period on 1.5 hours, again to insure no damage due to thermal stressing. Substrates were removed from the setup, excess glue was sanded away and the samples were cleaned and stored for future analysis. For a detailed listing of the films deposited see Table 1.

Table 1. Listing of films Deposited. Two sets of the following films were deposited one on $LaAlO_3$ and one on $SrTiO_3$

Thickness LSM0 (nm)	Pulses for LSMO Deposition	Thickness BFO (nm)	Pulses for BFO Deposition	Order of layers on substrate (bottom/top)
0	0	150	10,580	BFO
150	10,580	150	10,580	BFO/LSMO
200	14,100	150	10,580	BFO/LSMO
250	17,630	150	10,580	BFO/LSMO
150	10,580	0	0	LSMO
150	10,580	150	10,580	LSMO/BFO
150	10,580	200	14,100	LSMO/BFO
150	10,580	250	17,630	LSMO/BFO

X-ray diffraction and reflectivity measurements were performed on the manufactured samples using the Rigaku-ATXG diffractometer at the NU X-Ray Facility. For XRD analysis the diffractometer was in the slit collimation geometry with S_1 set to 0.5 mm (h) $\times$ 2 mm (v) and S_2 set to 0.01 mm (h) $\times$ 2 mm (v) S_3 and R were replaced with a soller slit so only peaks from the film, not the substrate, were seen. Omega was locked at 0.5^o and 2Theta was scanned from 20^o to 60^o. For XRR The diffractometer was in the GE111 Crystal geometry with S_1 set to 0.5 mm (h) $\times$ 2 mm (v), S_2 set to 0.01 mm (h) $\times$ 2 mm (v), S_3 set to 0.2 mm (h) $\times$ 5 mm (v), and R = 0.2 mm (h). The incident beam flux was 2.1×10^6 photons/sec. The step size for our scans was 0.001^o. Data was fit using the Motofit package available within IGOR thin film analysis software.

TEM imaging and XPS analysis were performed by outside technicians. A TEM sample was made from the 150nm_BFO_$LaAlO_3$, and was analyzed by Riad Alzghier of the Laboratory for Oxide Research and Education (LORE). XPS analysis was performed on 150nm_BFO_$SrTiO_3$ films by Ke-Bin Low of the Electron Microscopy Service at the University of Illinois at Chicago.

Results –

1A) 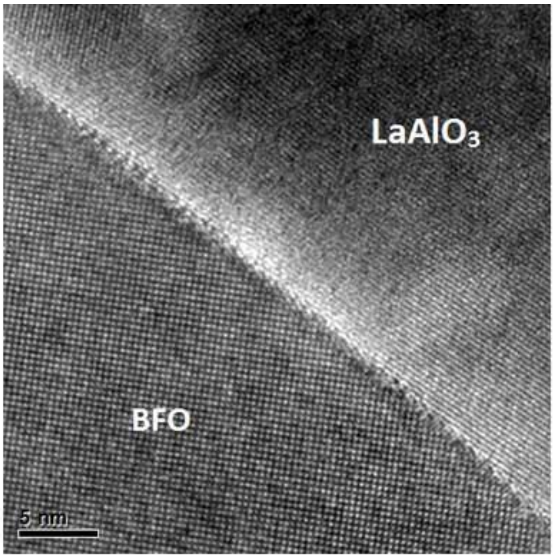

1B) 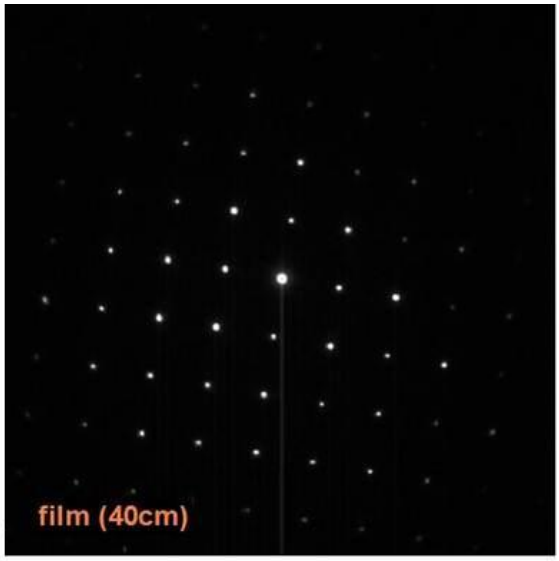

Fig 1, A and B. 1A) is a normal contrast images of the 150nm_BFO_$LaAlO_3$ film. 1B) is an electron diffraction pattern for the 150nm_BFO_$LaAlO_3$ film.

The TEM images in Fig 1A demonstrate that BFO films deposited by PLD are highly crystalline. The structure of the BFO film and the $LaAlO_3$ substrates is highly ordered. There are no visible grain boundaries in the film or substrate so it is possible that this is a single crystal film. This observation is supported by the electron diffraction pattern shown in Fig 1B which indicates that there is only one crystalline phase in the BFO layer. Additional TEM analysis indicates that the BFO layer is approximately 300 nm thick, twice the anticipated thickness. This may be a result of measuring growth rate only with LSMO, it was assumed that this value could be applied to BFO as BFO and LSMO have the same perovskite structure however TEM data demonstrates otherwise. It is important to note that TEM data is highly localized, and only samples a small portion of the surface, therefore, on the whole, film characteristics may deviate from the results pictured here.

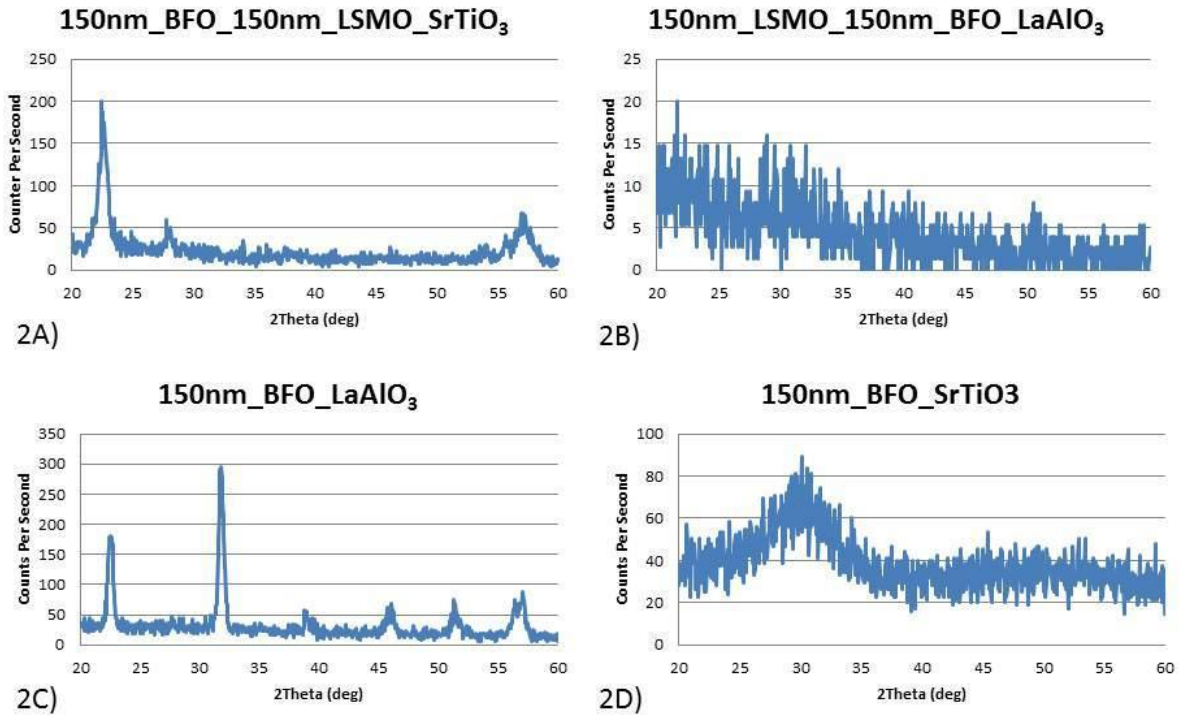

Fig 2, A-D. 2A) shows XRD data for a 150nm_BFO_150nm_LSMO_$SrTiO_3$ film that is approaching single crystal. 2B) shows data for an amorphous film of 150nm_LSMO_150nm_BFO_$LaAlO_3$. 2C) shoes data for a polycrystalline film of 150nm_BFO_$LaAlO_3$. 2D) shows data for a nanocrystaline film of 150nm_BFO_SrTiO3.

XRD analysis indicates that 9 of the 16 films deposited are amorphous as is the case for the 150nm_LSMO_150nm_BFI_$LaAlO_3$ film in Fig 2B , and five are nanocrystalline as with the 150nm_BFO_$SrTiO_3$ film shown in figure 2D. Nanocrystalline films have very small crystalline domains, on the order of 5 nm to 10 nm. There were two films that demonstrated crystalline order however. Fig 2C shows that the 150nm_BFO_$LaAlO_3$ film is polycrystalline in agreement with the TEM data for that film (Figs. 1). Finally, the 150nm_BFO_150nm_LSMO_$SrTiO_3$ film, XRD data shown in Fig 2A, is the highest quality film deposited. There is a sharp diffraction peak centered on 22.5^o and two minor peaks centerd around 27.8^o and 57.0^o respectively, which implies the film is approaching single crystal order. The 150nm_BFO_150nm_LSMO_$SrTiO_3$ film is a multilayer so the small peaks at high angles could be a result of the lower layer of the film not multiple crystalline phases.

Table 2. Size of crystallites in nanocrystalline films

Film	θ (radians)	B(2θ) (radians)	Crystallite Width (nm)
150nm_BFO_$SrTiO_3$	0.263	0.111	5
150nm_LSMO_$SrTiO_3$	0.256	0.0803	8
150nm_BFO_150nm_LSMO_$LaAlO_3$	0.265	0.111	5
200nm_BFO_150nm_LSMO_$SrTiO_3$	0.259	0.0986	6
250nm_LSMO_150nm_BFO_$SrTiO_3$	0.254	0.116	5

To further analyze the nanocrystalline the Scherrer Equation, shown below, was used to determine the size of the crystallites.

$$B(2\theta) = \frac{K\lambda}{Lcos\theta}$$

B(2θ) = Peak Width (radians)

λ = 0.1542 nm

L = Crystallite Width (nm)

θ = d-spacing (radians)

K = Scherrer Constant (Assumed to be 1)

The Scherrer Equation relates peak width, B(2θ), to crystallite size, L. After analyzing the data in Table 2, it was determined that the crystallites in the nanocrystalline samples range in size from 5 nm to 8 nm

approximately. The average crystallite size is 5.8 nm, rather large crystallites for nanocrystalline films. However, these values are tentative estimates, as the data has not been corrected to account for peak widening resulting from instrumentation, and not the film itself.

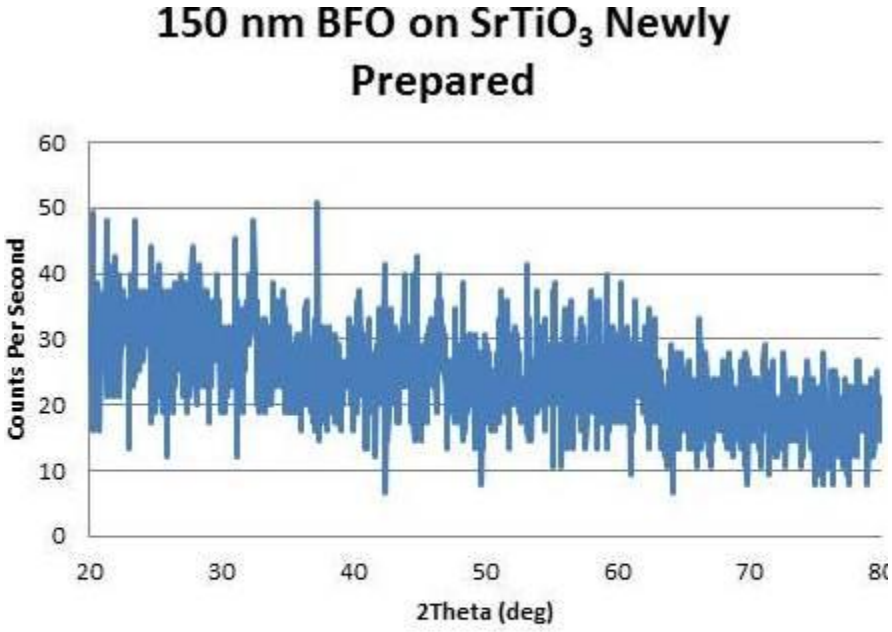

Fig 3. XRD data for the 150nm_BFO_$SrTiO_3$ prespared using alternate experimental procedure

To determine if the poor structure of the films was a result of the deposition process a new 150nm_BFO_$SrTiO_3$ sample was deposited using an alternate deposition process. The deposition temperature and pressure and the cooling/annealing temperature and pressure were changed. In this case the substrate was held at 670^{o} C during deposition, and the O_2 background pressure was held at $2*10^{-2}$ Torr. When deposition finished the oxygen background pressure was increased to 700 Torr. The sample was then cooled to 390^{o} C and held at that temperature for 1 hour to anneal, an additional step to ensure oxygen was not diffusing out of the film. Following annealing the film was removed from the PLD setup and analyzed via XRD as shown in Fig 3. The resulting data had no clear features indicating it

might be amorphous and of lower quality than the original film. To further understanding of what was going on this new film was subsequently analyzed by XPS, these results will be discussed later.

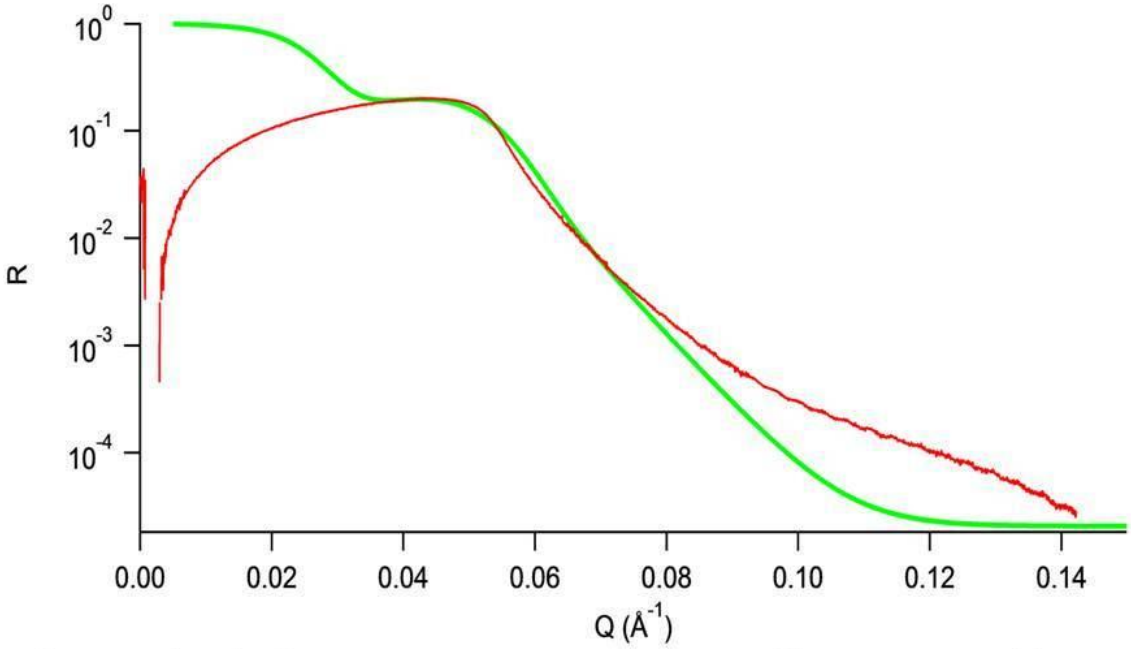

Fig 4. XRR data for the 150nm_BFO_150nm_LSMO_$SrTiO_3$ films, experimental data in red, fit data in green. R refers to the (measured beam intensity)/(Incident Beam Intensity). Q denotes reciprocal space.

.

Table 3. Thicknesses, scattering length densities (SLD), and roughnesses as determined by fitting XRR data for the 150nm_BFO_150nm_LSMO_$SrTiO_3$ film.

Layer	Thickness (Å)	SLD (Real)	SLD (Imaginary)	Roughness (Å)
Air	INF	0	0	0
Residue	84	$4.27*10^{-6}$	$3.32*10^{-8}$	30
BFO	1450	$6.57*10^{-5}$	$7.90*10^{-6}$	78
LSMO	1550	$5.09*10^{-5}$	$1.59*10^{-5}$	51
$SrTiO_3$ Substrate	INF	$4.49*10^{-5}$	$1.95*10^{-6}$	50

XRR did not afford much valuable information. The films were too rough to accurately model the extremely fine oscillations at high Q values seen in Fig 4. Of particular interest is the gradual decline in R which is very indicative of a high roughness film. Additionally the intensity of the X-rays used for XRR analysis was particularly low washing out R oscillations which are usually very prominent, but are barely visible in the XRR data. As a result this model does not provide accurate thickness information since the roughness was too high and the films were possibly too thick. Finally the most accurate model includes a high density, high roughness surface layer. This is not unphysical as the samples could not be fully cleaned before analysis as washing might have damaged the films. The upper layer is likely a combination of organic residue and possibly silver particles from the adhesive used to attach the substrate to the deposition stage which remained on the surface after sonication. However, as of yet the fit is not of sufficient quality to draw specific conclusions.

Table 4. XPS Results for original 150nm_BFO_$SrTiO_3$: Proper Stoichiometry Observed

Peak	Position BE (eV)	FWHM (eV)	Raw Area (CPS)	RSF	Atomic Mass	Atomic Conc. (%)	Mass Conc. (%)
Bi 4f	156	2.767	1302850	9.140	208.98	21	68
Fe 2p	708	4.572	378805.0	2.957	55.846	19	17
O 1s	527	3.162	318230.0	0.780	15.99	60	15

XPS analysis confirmed shown in Table 4 confirms that using the original deposition procedure, the stoichiometry of the deposited film roughly matched the stoichiometry of the starting target material. In spite of this, there is an observed Iron deficiency in the sample prepared using the new technique

described earlier. This discrepancy needs to be studied further to realize stoichiometric films. It is possible this deficiency caused the new sample to appear amorphous in the XRD data in Fig 21. XPS is a surface sensitive technique, only sampling the top several nanometers of a film so it is possible that stoichiometry deviations may not persist as the sampling depth is increased.

Conclusion/Discussion – In conclusion, while the films deposited were not epitaxial there is evidence that several of the films are highly crystalline. However there were a number of amorphous and nanocrystalline samples indicating problems during deposition. In order to identify the problem, an alternative experimental procedure was used to deposit a film to test this hypothesis, but the resulting film had abnormal stoichiometry deviations and no conclusions could be drawn. It was observed that PLD in an O_2 background preserves stoichiometry when depositing complex oxides. Finally, XRR data indicated films have high roughness and the model is incapable of providing accurate thickness data.

It is clear that the deposition process for LSMO and BFO has to be optimized to realize epitaxial growth. It is believed that low film quality is a result of the diffusion of oxygen out of LSMO and BFO during cooling. The formation of oxygen vacancies in the film results in the creation of multiple crystalline phases and may even result in metal precipitates like iron or bismuth. It would be advantageous, in the future, to experiment with raising oxygen pressure during cooling. This new procedure was attempted, but the resulting film was not suitable for use due to an iron deficiency. It may also be worthwhile to check the stoichiometry of the targets used as they are old and have been used multiple times. It is possible there are defects in the targets which are affecting the structure of the deposited films.

To close, while epitaxial multilayers of BFO and LSMO were not successfully deposited several key points were confirmed. Pulsed Laser deposition is capable of preserving stoichiometry and producing crystalline growth when depositing complex oxides. In the future it will be possible to refine deposition parameters to ensure epitaxial growth. One just needs to continue manipulating the O_2

background pressure and deposition and annealing temperatures and times. Additionally, in the future the targets used for deposition should be examined to ensure damage to the starting material is not affecting the deposited films. This study will provide guidance for future experiments on multilayers of BFO and LSMO.

Acknowledgements – The financial support from the National Science Foundation, EEC-NSF Grant # 1062943 is gratefully acknowledged. I would like to thank Professors Jursich and Takoudis for organizing the REU Program. I would also like to thank the LORE lab in general and Professor Jeremiah Abiade specifically for providing me with the opportunity to work in their lab.

Sources –

[1]P.S. Sankara Rama Krishnan, M. Arredondo, M. Saunders, Q. M. Ramase, M. Valanoor: 'Microstructural analysis of interfaces in a ferromagnetic-multiferroic epitaxial heterostructure', J. Appl. Phys., 2011, **109** 034103 (2011), 1-7.

[2]L. W. Martin, Y-H. Chu, M. b. Holcomb, M. Huijben. P. Yu, S-J. Han, D. Lee, S. X. Wang, R. Ramesh: 'Nanoscale Control of Exchange Bias with BiFeO3 Thin Films', Nano Letters, 2008, Vol. 8, No. 7, 2050-2055.

[3]X. Ke, L. J. Belenkey, C. B. Eom, M. S. Rzchowski: 'Antiferromagnetic exchange-bias in epitaxial ferromagnetic La0.67Sr0.33MnO3 /SrRuO3 bilayers', J. Appl. Phys., 2005, **97** 10k115 (2005), 1-3.

[4]M. Kharrasov, I. Kyzyrgulov, F. Iskahkov: 'Exchange enhancement of the magnetoelastic interaction in a LaMnO₃ crystal', Doklady Physics, 2003, Vol. 48, No. 9, 499-500.

[5]S. Habouti, R. K. Shiva, C-H. Solterbeck, M. Es-Souni, V. Zaporojtcheko: 'La0.8Sr0.2MnO3 buffer layer effects on microstructure, leakage current, polarization, and magnetic properties of BiFeO3 thin films', J. Appl. Phys., 2007, **102** 044113 (2007), 1-6.

[6]Esteve, D., Postava, K., Gogol, P., Niu, G., Vilquin, B. and Lecoeur, P. (2010), *In situ* monitoring of La0.67Sr0.33MnO3 monolayers grown by pulsed laser deposition. Phys. Status Solidi B, 247: 1956–1959. doi: 10.1002/pssb.200983960

[7]G-Z. Liu, C. Wang, C-C. Wang, J. Qiu, M. He, J. Xing, K-J Jin, H-B Lu, G-Z. Yang: 'Effects of interfacial polarization on the dielectric properties of $BiFeO_3$ thin film capacitors', Appl. Phys Lett., 2008. **92** 122903 (2008), 1-3

[8]D. B. Chrisey, G.K. Hubbler: 'Pulsed Laser Deposition of Thin Films', 13-56; 1994, New York, John Wiley & Sons.